

# A Droplet Simulation using Front-Tracking Method on Unstructured Mesh

Rhotaek Jung<sup>1</sup> and Toru Sato

Department of Environmental and Ocean Engineering  
University of Tokyo  
7-3-1 Hongo, Bunkyo-ku, Tokyo 113-8656, Japan  
TEL/FAX : +81 3 5802 3374

[rtjung@triton.naoe.t.u-tokyo.ac.jp](mailto:rtjung@triton.naoe.t.u-tokyo.ac.jp), [sato@triton.naoe.t.u-tokyo.ac.jp](mailto:sato@triton.naoe.t.u-tokyo.ac.jp)

<sup>1</sup> Present Address : Earth Simulator Center, 3173-25 Showa-machi, Kanazawa-ku, Yokohama-city, Kanazawa-ku, Japan

To represent a moving droplet interface accurately, a front-tracking method with a re-mesh technique in three-dimensional unstructured meshes is used. We investigated the drop motion according to the different Reynolds number in the liquid-liquid system. There are three regimes of the motion such as rectilinear regime, coexistence of both helical and zigzag motion, and mainly zigzag regime as increasing the Reynolds number. We compared experimental data of the silicon-water system to our simulation that provides more detail information of the relation between the rise velocity, trajectory, deformation, maximum velocity, and interface streamline when the droplet has zigzag motion.

## 1. Two-phase flow calculation

This work focuses on liquid-liquid two-phase system under gravitational fields. The liquid in disperse phase will start to move due to its buoyancy forces. The movement of the liquid-liquid interface is taken in account. The conservation equations on the moving mesh are derived by replacing the flux velocity in the convection term with the relative velocity.

In rising droplet simulations, to keep the position of a droplet at the origin, the negative value of acceleration  $\mathbf{a}$ , at its gravity center is added to the momentum equation as inertia as shown in below.

$$\begin{aligned} & \frac{d}{dt} \int \mathbf{u} dV + \int (\mathbf{u} - \mathbf{v}) \mathbf{u} \cdot \mathbf{n} dA \\ & = -\frac{1}{\mathbf{g}} \int p \mathbf{n} dA + \int \frac{1}{\mathbf{g}} \frac{Eo}{(OhRe)^2} \mathbf{g} dV + \frac{1}{Re} \frac{\mathbf{q}}{\mathbf{g}} \int [\nabla \mathbf{u} + (\nabla \mathbf{u})^T] \cdot \mathbf{n} dA + \mathbf{a} \end{aligned} \quad (1)$$

For droplet simulation, there are two kinds of Reynolds number that are  $Re$  as based on a reference velocity and  $Rn$  based on a droplet rise velocity. As one of output data, the  $Rn$  is reduced.  $Oh$  is the Ohnesorge number, and  $Eo$  is the Eötvös number,  $\mathbf{g}$  is density ratio, and  $\mathbf{q}$  is viscosity ratio.

In this study, the boundary condition of velocity at the interface is assumed by

$$\mathbf{m}_d \left. \frac{\partial u_n}{\partial n} \right|_d = \mathbf{m}_c \left. \frac{\partial u_n}{\partial n} \right|_c \quad \text{and} \quad \mathbf{m}_d \left. \frac{\partial u_t}{\partial n} \right|_d = \mathbf{m}_c \left. \frac{\partial u_t}{\partial n} \right|_c \quad (2)$$

From these relations, the interface velocity  $u_s$  is derived as follows

$$u_s = \frac{\mathbf{q} \frac{u_d}{\Delta l_d} + \frac{u_c}{\Delta l_c}}{\mathbf{q} \frac{1}{\Delta l_d} + \frac{1}{\Delta l_c}} \quad (3)$$

where, subscripts  $d$  and  $c$  are the disperse and continuous phase,

respectively. The  $u_d$  and  $u_c$  are the velocity at cell next to interface on each phase. The  $\Delta l_d$  and  $\Delta l_c$  are distance from interface to cell center location at each phase. As the boundary condition of pressure on the interface

$$p_d = p_c + \Delta p \quad \text{where,} \quad \Delta p = \frac{\mathbf{k}}{(Oh \cdot Re)^2} \quad (4)$$

The  $\Delta p$  is the pressure jump at interface. When calculating the pressure at cell placed inside of next cell to interface, the pressure outside of next cell to interface, whose pressure is added by  $\Delta p$ , is required.  $\mathbf{k}$  is the curvature. Since triangular prisms meshes are constructed near the interface, the form attached to the interface is a triangular. The curvature  $\mathbf{k}$  is treated by the gauss divergence theorem on a triangular face such as

$$\mathbf{k} = \nabla \cdot \mathbf{n} = \frac{1}{A} \int \mathbf{n} \cdot d\mathbf{l} \quad (5)$$

where,  $\mathbf{n}$  is outward unit vector normal to the interface, and  $d\mathbf{l}$  is the outward normal to the triangle edge vector on the interface plane and its value is the length of each edge and  $A$  is the area of the triangle.

Description of the moving interface is similar to that of wave height, which represents the free surface elevation

$$z = h(x, y, t) \quad (6)$$

Here,  $h$  is any scalar representing the position of the interface and a function of local coordinates  $(\mathbf{x}_1, \mathbf{x}_2, \mathbf{x}_3)$  and time  $t$  where  $\mathbf{x}_3$  in the direction is shown in Figure 1. Also we call that the  $h$  is "spine function". The spine function in this thesis is selected by generalized meaning of both radial direction moving and normal direction moving of the interface<sup>1</sup>.

In this study,  $h$  is the spine function, the distance between the

nodes on the interface and an arbitrary point along the  $x_3$  axis. As applying the kinematic condition, the following equation describing the local change of  $h$  through the direction of  $x_3$  can be written

$$\frac{\partial h}{\partial t} = \frac{1}{J} \left( U_3 \frac{\partial h}{\partial x_3} - U_1 \frac{\partial h}{\partial x_1} - U_2 \frac{\partial h}{\partial x_2} \right) \quad \text{where, } U_i = u_i b_{ij} \quad (7)$$

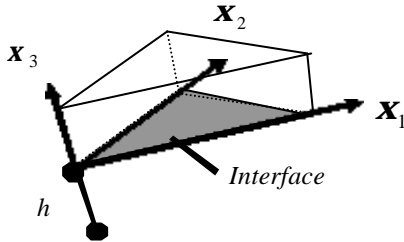


Figure 1. Definitions related to moving grids

The  $b_{ij}$  is the matrix to convert physical geometry information  $(x, y, z)$  into local coordinate system  $(x_1, x_2, x_3)$  and  $J$  is the Jacobian of matrix,  $u_i$  are fluid velocity. For stability of the equation (7), an upwind technique on convection term is adopted.

In the computational domain, triangular prisms of 15 layers are constructed at the interface and tetrahedrons are in the rest region as shown in Figure 2. A hybrid grid system comprising 297 nodes on solid surface and 590 triangular prisms is constructed by using a commercial mesh generator, ICEM-CFD.

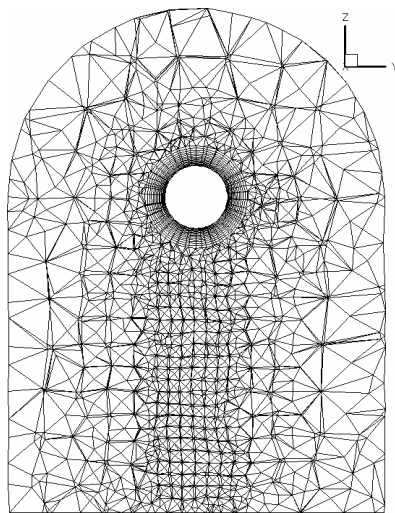


Figure 2. Hybrid unstructured mesh (Hybrid mesh in the drop is extracted for a simple view, total elements : 72247, number of triangular prism is 11800, and tetrahedron is 60447)

## 2. Results

At first, we simulate a free rising silicon droplet in water. The set Reynolds number is 826, when the diameter of the droplet is 0.00826m and reference rising velocity is 0.1m/s. The density and viscosity ratios of silicon-water system are 0.76 and 0.494, respectively. The Eötvös and Ohnesorge numbers in this simulation are 2.82 and 0.0015, respectively. The droplet is elliptically deformed and the mean aspect ratio  $E$  of the

deformation is about 0.7 ( $E$ =minor axis length/major axis length). In addition, it shows a zigzagging path in a vertical plane. The Reynolds number based on mean rise velocity  $U_R$  of about 0.15m/s is 1322, and the Strouhal number  $Sr = f d_0 / U_T$  is about 0.09. Figure 3(a) shows the rise velocity of the droplet and Figure 3(b) shows the trajectory of the droplet volume center in the  $xz$  and  $y-z$  planes, respectively. These trails show almost sinusoidal paths and have the period of about 0.6s. Two vertical guidelines are drawn at  $T=12.8$  and  $20.4$ , the time between which is one period for the zigzag path. Within the guidelines, nine specific times are chosen for displaying flow structures, i.e. A at  $T=12.8$ , B at  $T=14.0$ , C at  $T=15.0$ , D at  $T=15.8$ , E at  $T=17.2$ , F at  $T=18.4$ , G at  $T=19.2$ , H at  $T=19.8$ , and I at  $T=20.4$ . At the turning points (A, E, and I points) of the path, the droplet rise velocity has maxima and the aspect ratio has minima. This may be because the droplet suffers larger deformation due to high pressure at the top stagnation corresponding to the maximum velocity. It is obvious that the variations of the rise velocity and the aspect ratio have two main periods within one zigzagging motion of the trajectory. It is thought that producing large vorticity causes large drag and that the elliptical shape does not delay the rise speed.

The changes in shape oscillation of the droplet with comparison to experimental visualization are shown in Figure 4. The various shape deformations are similar to the experiments done by Imamura and Katayama<sup>2</sup> although the eye directions in the experiment and in the computation are not the same. The minor axis of the elliptical droplet is seemed to fit to the path direction.

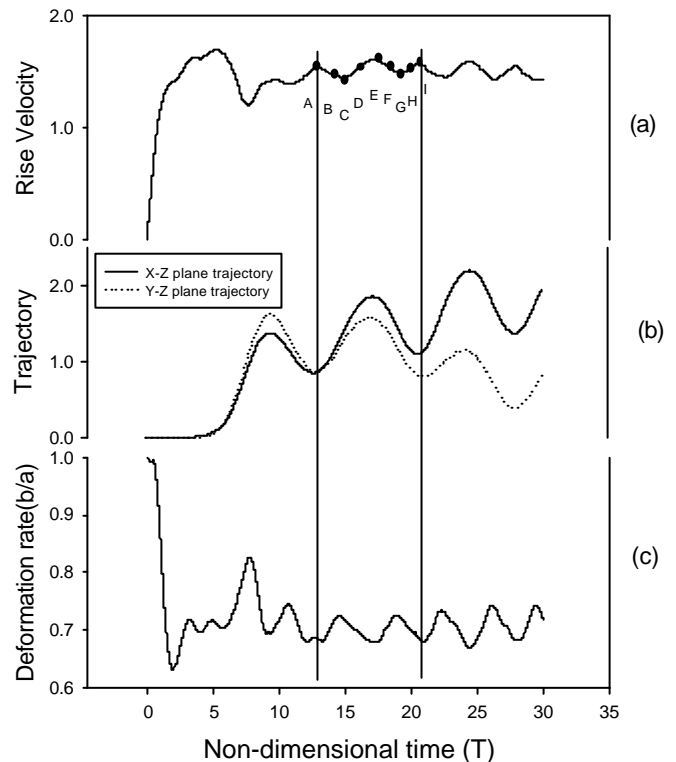


Figure 3. Variation of rise velocity (a), droplet path in  $x-z$  and  $y-z$  plane (b), aspect ratio (c). (Point A indicates 12.8T, B is 14.0T, C is 15.0T, D is 15.8T, E is 17.2T, F is 17.2T, G is 18.4T, H is 19.2T, and I is 19.8T for 1 zigzagging motion). The Reynolds number is about 1322 and the Ohnesorge number is 0.0015.

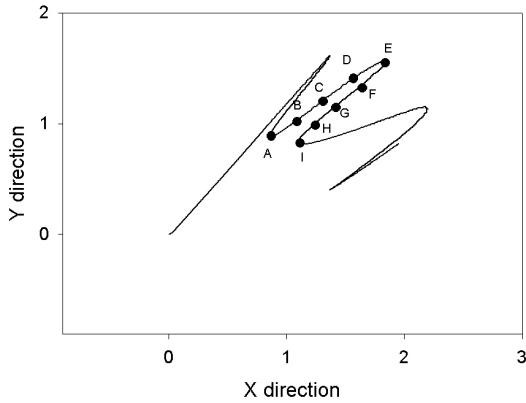


Figure 4. A droplet trajectory on X-Y plane (starting from 0,0). The alphabet letter on the line shows the same meaning of the description in Figure 3.  $Rn$  is about 1322 and  $Oh=0.0015$ .

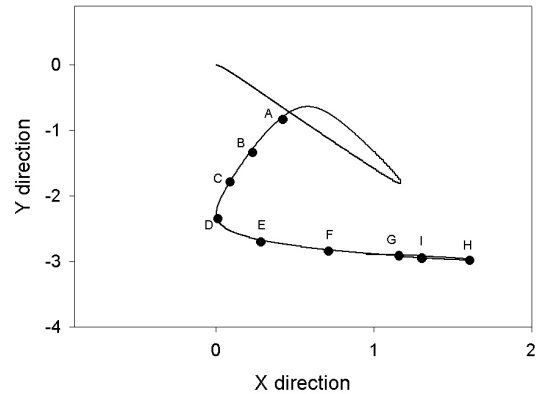


Figure 6. A droplet trajectory on X-Y plane (starting from 0,0). (A indicates 17.4T, B is 18.6T, C is 20.0T, D is 21.6T, E is 23.0T, F is 24.0T, G is 25.4T, H is 26.8T, and I is 28.0T for helical motion).  $Rn$  is about 650 and  $Oh=0.00187$ .

Experiments $Rn \approx 1479$	Period	Simulations $Rn \approx 1322$
	2T/9	
	4T/9	
	6T/9	
	7T/9	
	8T/9	
	T	

Figure 5. Comparison of droplet deformation experiments and present simulations in silicon-water system: T is a period of path. Photo by Imamura and Katayama<sup>(2)</sup>.

Next, we decreased the Reynolds number. The set Reynolds number is 500, when the diameter of the droplet is 0.005m and reference rising velocity of 0.1m/s. The density and viscosity ratios of silicon-water system are the same as those in the case of at  $Rn=1322$ , 0.76 and 0.494, respectively. The Eötvös and Ohnesorge numbers in this simulation are 1.03 and 0.00187, respectively. The Reynolds number based on mean rise velocity  $U_R$  of about 0.13m/s is about 650. The simulated results on this Reynolds number give the coexistence of both helical and zigzag motion. In the case of air bubble motion, Clift<sup>(3)</sup> suggested that there are five types of motion such as rectilinear ( $Rn < 565$ ,  $E > 0.8$ ), helical ( $565 < Rn < 880$ ,  $0.5 < E < 0.8$ ), and zigzag on a plane then helical ( $880 < Rn < 1350$ ,  $0.36 < E < 0.5$ ), zigzag on a plane ( $1350 < Rn < 1510$ ,  $0.28 < E < 0.36$ ) and rectilinear but with rocking ( $1510 < Rn < 4700$ ,  $0.23 < E < 0.28$ ), as increasing the Reynolds number. Since the two-phase system is different, air-liquid and liquid-liquid, the trend is not expected to be the same. In our simulation at about Reynolds number of about 650, two phenomena are shown in Figure 6 although the first one may be still developing. Nine specific moments are taken for visualizing the time evolution of flow structure, i.e. A at  $T=17.4$ , B at  $T=18.6$ , C at  $T=20.0$ , D at  $T=21.6$ , E at  $T=23.0$ , F at  $T=24.0$ , G at  $T=25.4$ , H at  $T=26.8$ , and I at  $T=28.0$ . From A to F on the trajectory, there is a helical path, while from F to I, there is a zigzag path.

We also simulated a droplet of the rectilinear motion. The set Reynolds number is 270, when the diameter of the droplet is 0.0027m and reference rising velocity is 0.1m/s. The rise velocity comes to steady state and the movement of droplet forms the rectilinear motion.

### 3. Conclusions

When the droplet locates at the turning point, the value of vorticity around separate line is the smallest. This means that vortex shedding happens at this moment, so that the rise velocity of the droplet increases rapidly and the droplet rises vertically. The zigzag motion is driven by pressure unevenly distributed on the rear surface of the droplet.

A vortex pair seems to correspond to the helical path. Instantaneous streamlines explain the rise velocity drop, as is mentioned in the case at  $Rn=1322$  on the droplet surface. Below the stagnation, there is almost symmetric circulation pair. At  $T=24.0$  and  $T=28.0$  in Figure 6, symmetric contour-rotating circulation pairs are observed. Between these times the point H, the zigzag turning, exists. We presume that the intensive

asymmetric circulation pair causes the helical motion and that, once the pair becomes symmetric, the motion changes to be steady zigzag on a plane.

#### **4. Reference**

- (1) Mashayek, F. and Ashgriz, N., (1995), "A Spine-Flux Method for Simulating Free Surface Flows", *Journal of Computational Physics*, Vo l. 122, pp. 367-379
- (2) Imamura K. and Katayama, T. (1999), "Study of droplet interface movement and dissolution in liquid-liquid two-phase flow", Undergraduate thesis, Dept. of Environmental and Ocean Engineering, University of Tokyo
- (3) Clift, R., Grace, J. R., and Weber, M. E. (1978), "Bubbles, Drops and Particles", Academic Press